IRON-RICH HALLOYSITE(10Å) WITH CRUMPLED LAMELLAR MORPHOLOGY FROM HOKKAIDO, JAPAN

Key Words—Halloysite, Electron microscopy, Morphology, Pumice, X-ray powder diffraction.

Halloysite is a kaolin-group clay mineral which is characterized by a diversity of morphology. Generally it occurs with a tubular morphology, but spheroidal halloysite particles are also common in weathered volcanic ashes and pumices. In addition, 'tabular' halloysite was found in Texas soils by Kunze and Bradley (1964) and Carson and Kunze (1970). Carson and Kunze (1970) also reported similar material in soils of Florida and Guatemala. Recently, platy halloysites with rolled edges were reported by Nagasawa and Miyazaki (1976) and Wilke *et al.* (1978). The present paper reports a morphologically new type of halloysite that displays a unique crumpled, lamellar morphology.

MATERIALS AND METHODS

Samples were collected from the weathered Tarumae d_2 pumice bed at Uenae, Tomakomai basin, Hokkaido, Japan,
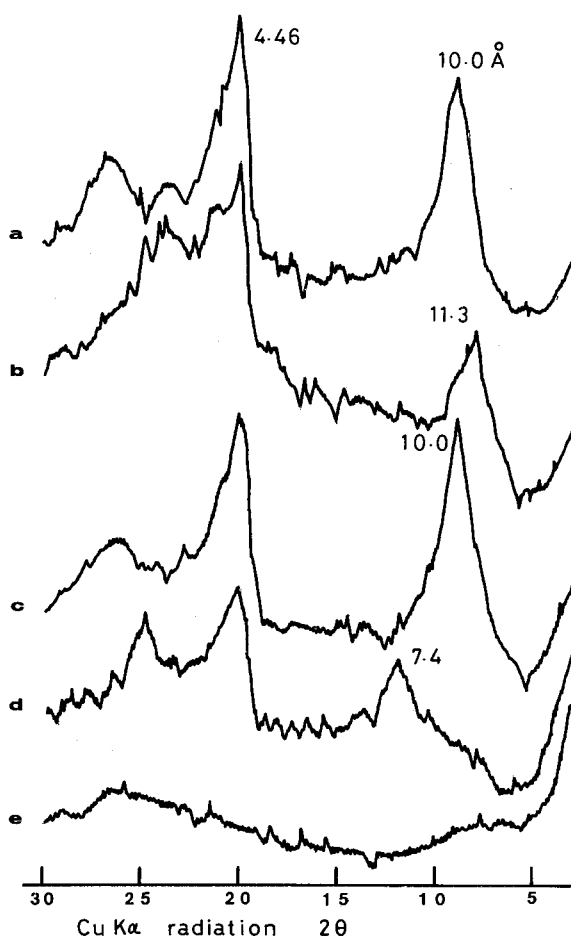

Figure 1. X-ray powder diffraction patterns of halloysite, Hokkaido, Japan: (a) Mg-saturated and air-dried. (b) Mg-saturated and glycerol solvated. (c) K-saturated and air-dried. (d) K-saturated and heated at 300°C. (e) K-saturated and heated at 550°C.

at a depth of 120–150 cm from the present surface. The samples were stored at a field moisture content in a stopped polyethylene bottle. The pumice was derived from the Tarumae volcano and is augite-hyperthene andesitic in composition (Ishii and Kondo, 1962). The C^{14} age of a charred wood fragment at the bottom of the bed was estimated to be 8490 ± 50 years B.P. (Sato, 1971). The halloysite occurs as yellowish brown clayey patches, nearly at the bottom of the pumice bed. The surrounding pumice grains are relatively hard and apparently less weathered. The pumice structure remains in the weathered portion, indicating that the halloysite formed by differential weathering of the pumice.

The undried bulk clay was gently pulverized in water, and the pH of the resulting suspension was adjusted to 10 with NaOH. The clay (<2-μm fraction) was dispersed with the aid of an ultrasonic treatment and collected by sedimentation. Part of the clay separate was stored as such for electron microscopy and cation-exchange capacity (CEC) determination, and the remainder was successively treated with dithionite-citrate and 2% Na_2CO_3 solutions to remove free iron oxides and the adsorbed citrate, respectively. Part of the treated clay was kept as a suspension for X-ray powder diffraction (XRD) analysis and electron microscopy. The remainder was successively washed with a water-methanol solution, methanol and acetone, and then air-dried.

Total elemental analysis of the air-dried clay was carried out according to the procedure described by Aomine and Harada (1971). Ferrous ion was not determined separately, and the iron content is therefore expressed as percent Fe_2O_3. XRD patterns were obtained from K- and Mg-saturated samples of the clay oriented on glass slides using CuK_α radiation. Infrared (IR) absorption spectra were recorded with KBr pellets. Differential thermal analysis (DTA) was carried out on a 30-mg sample at a heating rate of 20°C/min. Electron micrographs were obtained from specimens prepared by air-drying a drop of the clay suspension on a collodion film or on a plastic microgrid. CEC was determined on the clay without any treat-
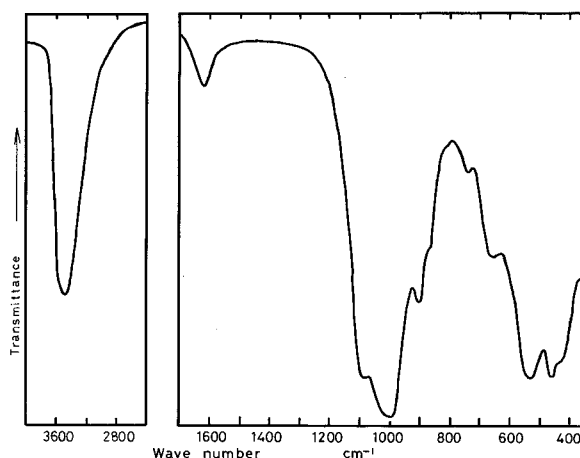

Figure 2. Infrared spectrum of halloysite, Hokkaido, Japan. Transmittance increases upward along the ordinate for each spectrum.
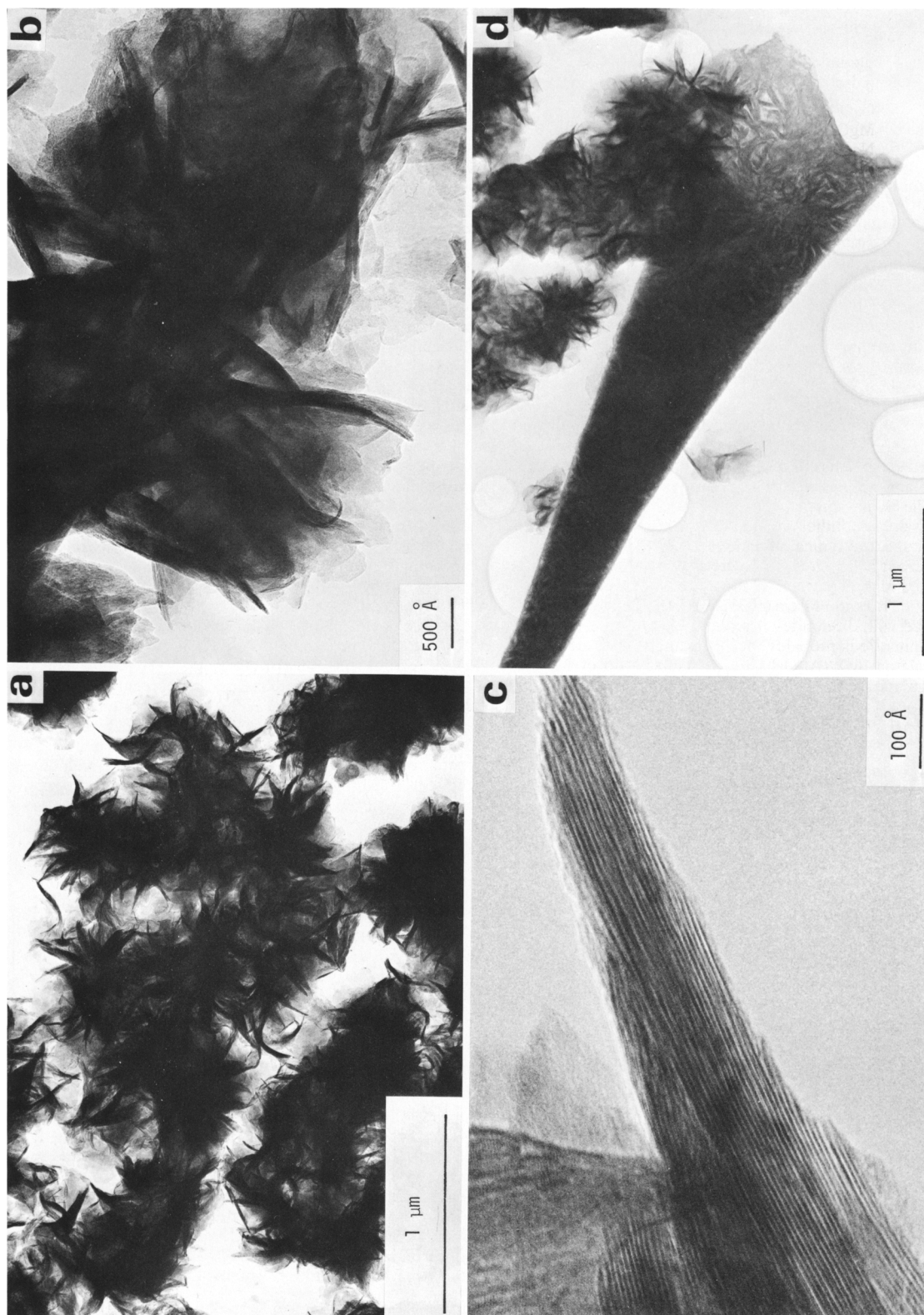
315

Figure 3.   Transmission electron micrographs of halloysite, Hokkaido, Japan. (a) Halloysite particles with crumpled lamellar morphology; (b) very thin flakes constituting a particle; (c) lattice images observed on a protruding edge; (d) a particle with sharp edges replaced with the halloysite.

Table 1. Chemical composition of halloysite, Hokkaido, Japan, treated with dithionite-citrate and 2% Na_2CO_3 solutions.

SiO_2	44.7
Al_2O_3	28.1
Fe_2O_3	12.8
CaO	trace
MgO	0.1
Na_2O	1.7
K_2O	trace
MnO	trace
H_2O (+)	13.3
Total	100.7

(% by weight on the oven-dried material.)

ment according to the procedure described by Aomine and Harada (1971).

RESULTS AND DISCUSSION

Figure 1 shows XRD patterns of the clay. The basal spacing of air-dried specimens (10.0 Å) expanded to 11.3 Å on glycerol solvation and collapsed to 7.4 Å on heating the sample at 300°C. The b_0 parameter calculated from the (060) spacing (1.49 Å) is 8.94 Å, indicating that the mineral is dioctahedral. These features are typical of halloysites.

The present halloysite is characterized by relatively low Al content and high Fe content compared with the data summarized by Weaver and Pollard (1973) (Table 1). Because the clay was treated with dithionite-citrate and 2% Na_2CO_3 solutions, the remaining Fe is probably located in the silicate structure. The calculated $SiO_2/(Al_2O_3 + Fe_2O_3)$ molar ratio of 2.09 indicates that most of Fe is in the octahedral position. The CEC of the clay without dithionite and 2% Na_2CO_3 treatments is 58.1 meq/100 g. This high CEC can be accounted for by assuming the substitution of ferrous ion for aluminum ions, providing layer charge.

Figure 2 shows the IR spectrum of the air-dried clay. An OH-stretching absorption band appears in the range 3700 to 2800 cm^{-1}. The absorption bands of structural OH groups of halloysite, which are usually observed in the range 3620–3700 cm^{-1}, were not resolved, presumably due to the overlapping of broad band of adsorbed water. With the exception of a shoulder at about 870 cm^{-1}, all other absorption bands are known in halloysite. Kunze and Bradley (1964) also observed this shoulder at 870 cm^{-1} for tabular halloysite and compared it with the absorption band at 860 cm^{-1} in nontronite. Serratosa (1960) assigned this band to a vibration involving hydroxyls bound to one aluminum and one iron.

The DTA pattern showed two endothermic peaks at 110° and 476°C and a weak exothermic peak at 863°C. Under the same conditions, a tubular halloysite of hydrothermal origin exhibited endothermic peaks at 80° and 540°C and an exothermic peak at 990°C.

Electron micrographs show that the halloysite occurs as crumpled lamellae which seem to be intergrown (Figure 3a, 3b). The edges of the lamellae are so thin that they are almost transparent to the electron beam (Figure 3b). At higher magnification, the regularly stratified lattice images with separations of 7 Å are visible on the protruding flakes (Figure 3c). The number of unit layers in a single lamella generally appears to be less than 30. The lamellae are gently curved, but concentric enrollment was not noted in the micrographs (Figure 3a, 3b). The sample without dithionite-citrate and 2% Na_2CO_3

treatments also displayed the same morphology, indicating that the morphology of the present halloysite (Figures 3a, 3b) is not an artefact caused by the treatments.

The most prominent structural feature of most halloysites is the concentric rolling of stacked silicate layers which results in tube-like or spheroidal morphology. The curvature of the silicate layers is usually explained in terms of the misfit in dimension between the tetrahedral and octahedral sheets and the weakness of interlayer bonding (Bates et al., 1950; Bates, 1959). The smaller curvature of lamellae of the present halloysite can be accounted for in a similar manner. The incorporation of iron in the octahedral sheet is a likely cause for an increase in its lateral dimensions and results in a decrease in the misfit between the tetrahedral and octahedral sheets. The invariably high iron content of tabular halloysites (Kunze and Bradley, 1964; Carson and Kunze, 1970) supports this view.

Allophane and imogolite, clays commonly derived from volcanic ejecta, were not detected in the present sample. On the other hand, the fine-sand fraction of the bulk sample contained abundant volcanic glass fragments with sharp edges. Many particles with similar sharp edges were also found in the silt and clay fractions. Most of these particles were found to be noncrystalline by electron diffraction. Some of these particles in the clay fraction were almost replaced with the aggregates of the lamellae (Figure 3d). The above observations suggest that this halloysite forms directly from volcanic glass.

ACKNOWLEDGMENT

Faculty of Agriculture   SHIN-ICHIRO WADA
Kyushu University 46   CHITOSHI MIZOTA
Fukuoka 812, Japan

REFERENCES

Aomine, S. and Harada, T. (1971) Laboratory Manual for Soils and Fertilizers: Yokendo, Tokyo, Japan, 17–19, 37–55.

Bates, T. F. (1959) Morphology and crystal chemistry of 1:1 layer lattice silicates: *Amer. Mineral.* **44**, 78–114.

Bates, T. F., Hildebrand, F. A., and Swineford, A. (1950) Morphology and structure of endelite and halloysite: *Amer. Mineral.* **35**, 463–484.

Carson, C. D. and Kunze, G. W. (1970) New occurrence of tabular halloysite: *Soil Sci. Soc. Amer. Proc.* **34**, 538–540.

Ishii, J. and Kondo, Y. (1962) Clay minerals of Quaternary volcanic ash and pumice deposits in Hokkaido: *Adv. Clay Sci.* **4**, 193–212.

Kunze, G. W. and Bradley, W. F. (1964) Occurrence of tabular halloysite in Texas soil: in *Clays and Clay Minerals, Proc. 12th Natl. Conf., Atlanta, Georgia, 1963*, W. F. Bradley, ed., Pergamon Press, New York, 523–527.

Nagasawa, K. and Miyazaki, S. (1976) Mineralogical properties of halloysites as related to its genesis: *Proc. Int. Clay Conf., Mexico City, 1975*, S. W. Bailey, ed., Applied Publishing, Wilmette, Illinois, 257–265.

Sato, H. (1971) C^{14} age of Tarumae volcanic ash d member: *Earth Sci.* **25**, 185–186.

Serratosa, J. M. (1960) Dehydration studies by infrared spectroscopy: *Amer. Mineral.* **45**, 1101–1104.

Weaver, C. E. and Pollard, L. D. (1973) *The Chemistry of Clay Minerals:* Elsevier, Amsterdam, 150–151.

Wilke, B. M., Schwertmann, U., and Murad, E. (1978) An occurrence of polymorphic halloysite in granite saprolite of the Bayerischer Wald, Germany: *Clay Miner.* **13**, 66–67.